



Research article

A canine thromboembolic model of anterior circulation large vessel occlusion stroke



Amanda S. Zakeri^a, Debra G. Wheeler^{a,*}, Allyson Huttinger^a, Arianna Carfora^a, Aarushi Kini^a, Taggart Stork^a, Simon Yacoub^a, Cole Anderson^a, Matthew Joseph^b, Mohammed T. Shujaat^c, Shahid M. Nimjee^a

^a Department of Neurosurgery, The Ohio State University Medical Center, Columbus, OH, USA

^b Dorothy M. Davis Heart and Lung Research Institute, The Ohio State University Medical Center, Columbus, OH, USA

^c Department of Radiology, The Ohio State University Medical Center, Columbus, OH, USA

ARTICLE INFO

Keywords:

Stroke
Middle cerebral artery occlusion
Canine model

ABSTRACT

Purpose: To develop a large animal preclinical model of thromboembolic stroke with stable, protracted large vessel occlusion (LVO) utilizing an autologous clot.

Materials and methods: A reproducible canine model of large vessel occlusion stroke was established by endovascular placement of an autologous clot into the middle cerebral artery (MCA) of six adult hounds and confirmed using digital subtraction angiography (DSA). Infarct volume and evidence of hemorrhage were determined by magnetic resonance imaging (MRI) 7 h after occlusion and Thrombolysis in Cerebral Infarction scale (TICI) was assessed before and after clot placement and at 1, 6, 7, and 9 h after middle cerebral artery occlusion (MCAO). Heart rate (HR) and blood pressure (BP) were monitored continuously and invasively through an arterial sheath throughout the procedures and complete blood count and blood gas analysis completed at time of sacrifice. Histopathological findings at time of sacrifice were used to confirm stroke volume and hemorrhage.

Results: MCAO with resulting TICI 0 flow was observed in all six animals, verified by serial DSA, and lack of collateral flow persisted for 9 h after clot placement until time of sacrifice. The mean infarct volume was $47.0 \pm 6.7\%$ of the ipsilateral hemisphere and no events of spontaneous recanalization or clot autolysis were observed.

Conclusion: We demonstrate a thromboembolic canine model of MCAO that is both feasible and results in consistent infarct volumes to generate a clinically relevant LVO. This model is important to evaluate treatment of LVO in acute ischemic stroke (AIS) outside the established 4.5 h recombinant tissue plasminogen activator (rtPA) therapeutic window utilizing a prolonged occlusive thrombus.

1. Introduction

Acute ischemic strokes (AIS) are a leading cause of morbidity and mortality worldwide with ~80% being ischemic [1,2]. In the past two decades there have been significant advancements in stroke treatment including expansion of the use of rtPA to 4.5 h after last

* Corresponding author.

E-mail address: debra.wheeler@osumc.edu (D.G. Wheeler).

<https://doi.org/10.1016/j.heliyon.2023.e14692>

Received 28 November 2022; Received in revised form 1 March 2023; Accepted 15 March 2023

Available online 1 April 2023

2405-8440/© 2023 Published by Elsevier Ltd.

This is an open access article under the CC BY-NC-ND license

(<http://creativecommons.org/licenses/by-nc-nd/4.0/>).

known well and endovascular interventions including *trans*-arterial clot aspiration and mechanical retrieval. Translational research aimed at introducing novel devices and AIS therapeutics requires a large animal model to investigate the safety and efficacy of these interventions to recapitulate clinical AIS LVO and comparison with rTPA limitation necessitates demonstration of a protracted stable thrombus beyond 4.5 h. Among currently available large animal cerebral ischemia models, only rabbits, dogs, and non-human primates (NHP) are the only species suitable for LVO that do not necessitate a craniotomy and can be completed with an endovascular approach [3]. Canines and NHP are favored due to clinically comparable anatomy, with canines resulting in significantly lower experimental costs compared to NHP. Importantly, swine and ovis have a rete mirabile not present in humans, NHP, or canines [3]. This capillary network supplying the intracranial circulation makes endovascular access to the MCA challenging, if not impossible, and requires an invasive craniotomy. Recent reviews of animal models of stroke describe focal ischemia induced by thromboembolic occlusion as poorly reproducible with frequent spontaneous recirculation and high complication rates [4–6]. To that end, we describe a reproducible MCAO canine model of LVO stroke using endovascular placement of an autologous clot with stable occlusion over prolonged ischemic challenge.

2. Methods

2.1. Canine model of thromboembolic MCA occlusion

Six adult mongrel hounds (Oak Hill Genetics, Ewing, IL) were used to complete this study with a mean age of 13.4 months and mean weight of 26.2 kg (Table 1). All procedures were approved by The Ohio State University Institutional Animal Care and Use Committee and were performed in compliance with the Animal Welfare Act and the Guide for Care and Use of Laboratory Animals (NRC 2011). Feeding was restricted 12 h before anesthesia was induced. Animals received intramuscular acepromazine (0.2 mg/kg) prior to intubation. A 20-gauge catheter was placed in the cephalic vein and anesthesia was induced with intravenous administration of ketamine (10 mg/kg) and midazolam (0.025 mg/kg). Hounds were intubated and mechanically ventilated at 12 respirations per minute with constant flow anesthesia (2–3% isoflurane) and vitals continuously monitored. The equipment that recorded canine vitals was mobile with battery back-up (Passport, Datascope) and followed the animal during transport to and from MRI and long monitoring leads connected to the canines inside the MR imager. Animals were placed supine with the head slightly extended (Fig. 1A) in an inflated MRI compatible Hug-u-Vac (Surgical Positioning Systems, Sports Doc Inc, Salem, OR) which maintained body temperature at 37 ± 1 °C recorded with a rectal probe throughout the entire procedure. A cutdown was performed over the right femoral artery to insert a 7F arterial sheath via Seldinger technique. A 16 gauge angiocatheter was inserted into the right femoral vein to extract blood for autologous clot preparation, blood gas analysis (BGA), and complete blood count (CBC). To create the autologous clot, 5 mL of whole blood was drawn into a 5 mL BD Luer lock syringe and sat undisturbed in the syringe for 60 min prior to injection at room temperature. In the event target vessel access took longer than 60 min, the clot preparation was repeated. A tri-axial system involving a 7F arterial sheath, a 5F angled glide catheter and Echelon 10 microcatheter over a Synchro 2 softwire were used to access the internal carotid artery (ICA). A baseline DSA was then performed to include the carotid and intracranial circulation (OEC 9800 Cardiac Plus). At this time, the vasculature was pre-screened for tortuosity to determine whether the left or right MCA had the best access route for clot placement. Next the microcatheter was advanced through the vertebral artery to the posterior communicating artery to reach the MCA. The autologous clot was loaded into a high pressure syringe (Medallion, Merit Medical, South Jordan, UT), injected into the MCA, stabilized for 3 min, and followed by 1 mL of contrast (350 mg/I, Omnipaque, GE) to flush the remaining clot from the catheter. Injection stopped when the vessel was occluded, verified by additional fluoroscopy with contrast that did not pass the occlusion into the distal MCA. This process including clot injection, contrast and verification of occlusion was performed in approximately 5 min. If MCAO was not complete, additional clot and contrast was added. This was only necessary in one canine (#9155). Clot placement and complete MCA occlusion was confirmed from DSA with Thrombolysis in Cerebral Infarction scale (TICI) 0 flow and MCAO start time was recorded.

2.2. Six hours of occlusion was selected as it was outside the therapeutic window of rTPA treatment

After 6 h of ischemia, PBS, pH 7.4 was infused intravenously at 2 mL/min to replicate a therapeutic treatment before transport for MRI, a short 2–3 min drive from the angiography suite. The arterial sheath was left in place for additional injectable anesthesia during transport, if necessary, and to expedite return from imaging for sacrifice. Animals were sacrificed upon return from MRI after completion of final blood draws and DSA.

Table 1

Subject details.

Animal #	Sex	Age (mo)	Weight (kg)	Infarct Volume (%)	Heart Rate (bpm)	MAP (mmHg)
9155	F	15.5	23.0	42.25	78 ± 4	70 ± 7
9294	F	14.4	17.2	54.15	80 ± 6	46 ± 7
9397	M	13.6	33.2	49.18	125 ± 4	59 ± 6
9660	M	13.0	29.2	51.09	104 ± 5	94 ± 4
9735	M	12.1	28.4	37.57	90 ± 4	86 ± 8
9741	M	12.0	26.2	53.83	102 ± 10	83 ± 7

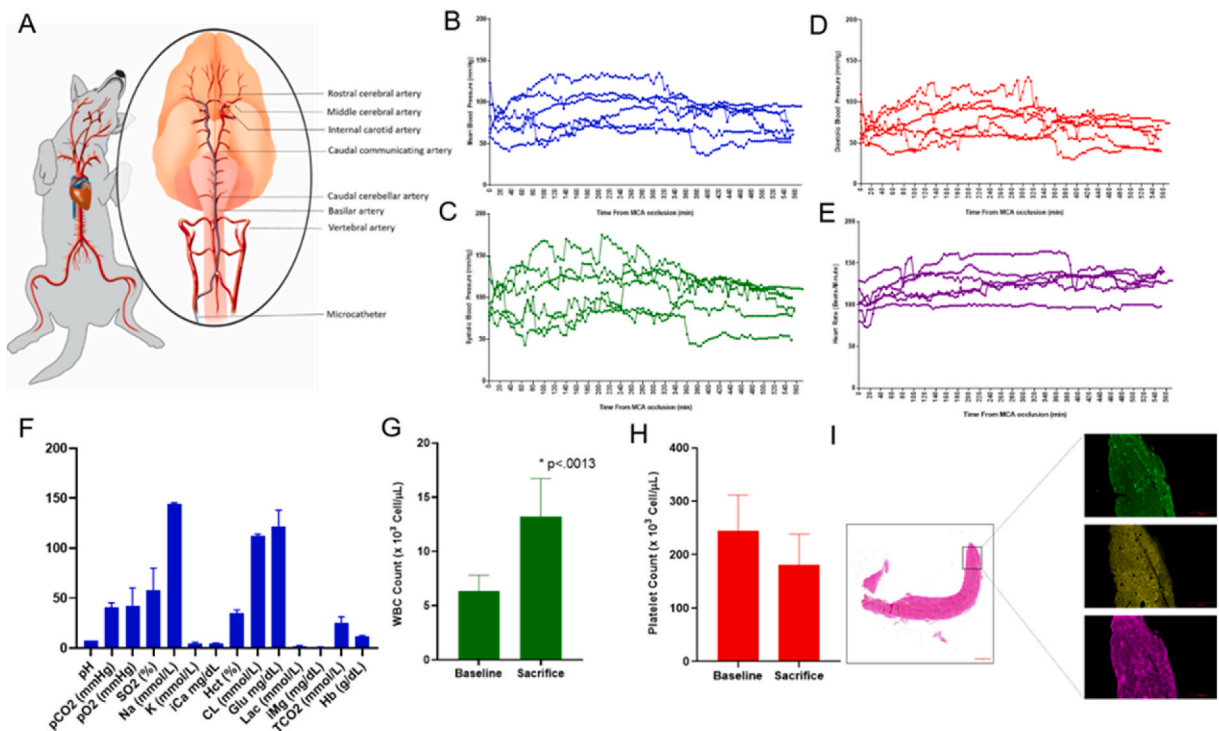


Fig. 1. Posterior access MCAO canine occlusion model. A. Animal positioning and views of arterial blood supply and microcatheter path (inset, blue) for autologous clot placement to the left middle cerebral artery. Mean (B), systolic (C), and (D) diastolic arterial blood pressure from clot placement to sacrifice in each of six hounds. E. Heart rate from clot placement to sacrifice in each of six hounds. F. Mean values \pm SD of all blood gas parameters measured at time of sacrifice, 9 h after MCAO initiation. G. White blood count at baseline ($6.33 \pm 1.49 \times 10^3$ cells/ul) and time of sacrifice ($13.24 \pm 3.48 \times 10^3$ cells/ul) showed significant increase 9 h after MCAO ($n = 6$, $p < .0013$). H. Platelet count at baseline ($243.8 \pm 67.7 \times 10^3$ cells/ul) and time of sacrifice ($181.2 \pm 57.1 \times 10^3$ cells/ul) were insignificant ($n = 6$, $p = .1137$). I. Representative autologous clot H&E staining at $10\times$ magnification (left) and insets of immunofluorescent staining for fibrinogen (green), platelets (yellow), and von Willebrand Factor (purple), 60 min after autologous whole blood draw ($n = 4$).

2.3. Imaging-magnetic resonance and TICI evaluation

MRI analysis of infarct volume, edema, and hemorrhage were performed by a blinded board certified neuroradiologist as previously described [7,8]. A Siemens Prisma 3 T MRI 60 cm bore scanner and a 32-channel head coil with enhanced parallel imaging were used to obtain canine brain images [7,8]. Localizer scans were first performed to acquire pilot images before anatomical imaging began. Image sequences acquired included diffusion weighted imaging (DWI), from which ADC (Apparent Diffusion Coefficient) maps were constructed to quantify the extent of injury on the DWI image, T2-weighted, Fluid Attenuated Inversion Recovery (FLAIR) and T2-weighted gradient echo images [7]. Hemorrhage, which was ruled out by T2-w FLAIR, is highly sensitive to detect sub arachnoid hemorrhage and acute cerebral venous sinus thrombosis which both appear hyperintense because T2 w FLAIR suppresses signal intensity of bulk water. This imaging is most sensitive in the acute stroke phase in the MCA, generally visible beginning 3–6 h post-stroke [9]. The system utilized to obtain the presented data has an integrated imaging system which allows faster scanning in optimal spatial and temporal resolutions with 80 mT/m gradients that generate high-quality T2-weighted, DWI and MR angiograms. Briefly, after localizer images, T2-weighted imaging was performed (Parameters: FOV = 130 mm, Matrix size = 320×320 , pixel size = 0.3×0.3 mm, Slice thickness = 3 mm, TR = 4s, FA = 180° , BW = 255 Hz/pixel, NEX = 2, TE = 75 ms, Resolution = 2.4615 pixels per mm), followed by FLAIR images for detection of edema. DWI sequences were used to detect acute ischemic strokes (Parameters: FOV = 149 mm \times 149 mm, Matrix size = 132×100 , pixel size = 0.3×0.3 mm, slice thickness = 4 mm, TR = 4.6s, FA = 90° , BW = 255 Hz/pixel, NEX = 1, TE = 86 ms, Resolution = 0.93 pixels per mm), confirmed by the generated ADC maps. DICOM images were transferred for post-processing, and infarct volumes were calculated using Horos open-source software based on OsiriX™. The calculation of hemispheric and infarct volumes was performed using manually drawn regions of interest (ROI) around the areas of infarct-related edema and diffusion restriction, measured per slice with the respective values multiplied by slice thickness to generate exact infarct volumes as previously published [7,8]. Thrombolysis in Cerebral Infarction scale (TICI) was assessed before and after clot placement and at 1, 6, 7, and 9 h after middle cerebral artery occlusion (MCAO) as previously described [10].

2.4. Hematoxylin and eosin (H&E) staining of canine brain

Brains were harvested at sacrifice and two medial sections were cut 4 mm thick. Briefly, one 4 mm section was fixed in 10% neutral buffered formalin for 7 days and embedded in paraffin. Each block was trimmed, leveled, and sectioned at 4 μ m on to 2'' \times 3'' glass slides. Slides were stained in Hematoxylin 560 for 8 min, differentiated with 1% acid alcohol for 1 s (s) three times and rinsed in water. Slides were blued in 1% ammonium hydroxide for 1s, rinsed for 2s with water, dehydrated in 70% ethanol for 1s twelve times and counterstained in eosin for 1 min. After dehydration in 95% ethanol for 1s twelve times followed by 100% ethanol, slides were cleared in xylene and coverslipped [7]. Slides were scanned at high resolution on a Zeiss Axioscan Z.1 and the same neuroradiologist who evaluated MR images compared percent infarction and identified hemorrhagic regions in the comparable MR scanned regions [7].

2.5. 2,3,5-Triphenyl-2H-tetrazolium chloride (TTC) staining of canine brain

The other 4 mm medial brain section which was harvested was immediately placed into 100 mL of 2% TTC in PBS, pH 7.4 warmed to 37 $^{\circ}$ C. After incubation in the dark at 37 $^{\circ}$ C for 20 min with inversion every 5 min, sections were cherry red and TTC solution replaced with 4% paraformaldehyde in PBS, pH 7.4, to optimize color contrast for 3 days at room temperature. After 3 days, slides were scanned at high resolution on a Zeiss Axioscan Z.1 and the same neuroradiologist who evaluated MR images in the comparable MR scanned regions [7].

2.6. Immunofluorescent staining of autologous clot preparations

In order to compare the composition of autologous clots placed endovascularly into the MCA, we prepared additional clots alongside injected clots and performed immunofluorescent staining for fibrinogen, platelets, and von Willebrand Factor (VWF) as previously published [11]. Briefly, the whole blood that had been extracted into a 5 mL BD Luer lock syringe sat undisturbed for 60 min prior to injection at room temperature. The clot was fixed in 4% paraformaldehyde in PBS, pH 7.4 for 24 h, embedded in paraffin and

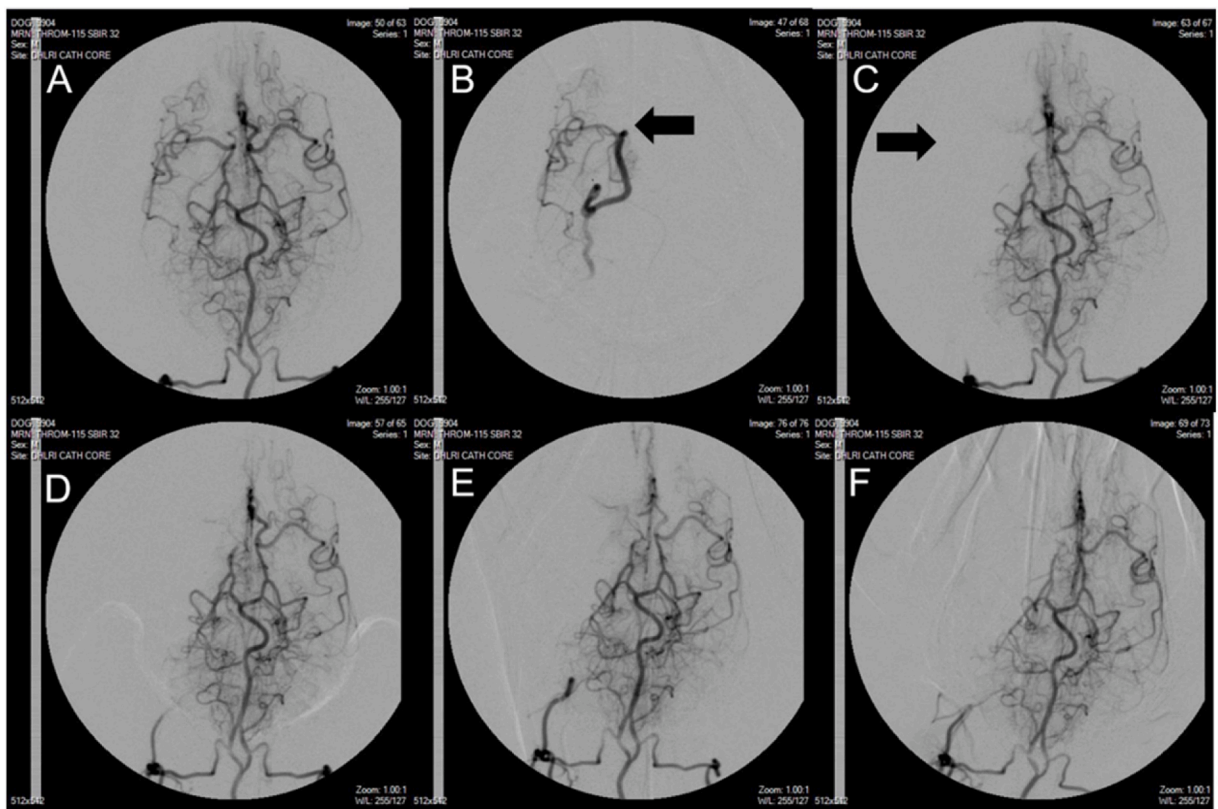


Fig. 2. Serial representative digital subtraction angiography (DSA) of intracranial arteries in MCAO model canine study. A. Baseline image demonstrating cerebrovascular anatomy of the hound. B. Location of microcatheter tip (arrow) immediately before clot placement. C. MCAO 3 min after clot placement with no collateral flow to MCA territory (arrow). D. Persistent localized lack of flow to MCA territory 6 h after occlusion. E. Last DSA demonstrating stable MCAO with no reflow immediately before transport to MRI facility 7 h after MCAO induction. F. Final DSA after MRI and return transport to angiography suite verifying stable MCAO 9 h after ischemic start. Microcatheter and contrast injection is at the bottom of the images to visualize the entire field of blood perfusion whereas it is placed at the MCA in B to visualize occlusion.

sectioned at 6 μm . One slide was stained with H&E and a second slide for immunofluorescence (IF). After antigen retrieval and blocking, slides were incubated with primary antibodies to fibrinogen (8.5 $\mu\text{g}/\text{mL}$; Dako, ref F011), VWF (15.5 $\mu\text{g}/\text{mL}$; Dako, ref A0082), and CD42b to identify platelets (2 $\mu\text{g}/\text{mL}$; Beckman Coulter, Sharon Hill, PA, ref IM0409). After secondary antibody, slides were counterstained with Hoechst 33,342 (10 $\mu\text{g}/\text{mL}$; Life Technologies, Carlsbad, CA) and mounted with Fluoromount G medium (Invitrogen, ref 00495802). Control slides were prepared simultaneously without primary antibodies to assess background and nonspecific binding. We visualized platelets, fibrinogen, and VWF with a Zeiss Axio Scan Z.1 using Orbit Image analysis software (www.orbit.bio). The software scans for the presence by color-based segmentation analysis and Image J was used to compare the component positive area staining as a percentage of the total area of the thrombus.

3. Results

Individual animal physiological parameters at baseline and infarct sizes measured with MRI have been included in [Table 1](#). Advancing the microcatheter through the vertebral artery to the posterior communicating artery to place an autologous clot into the MCA resulted in complete occlusion in all 6 hounds which persisted for 9 h ([Fig. 1A](#)). A repeated measure *t*-test of intraoperative heart rate, mean arterial pressure, systolic arterial pressure, and diastolic arterial pressure showed no significant changes between pre- and post-MCA occlusion ([Fig. 1B–E](#)). Parameters for all hounds included in standard blood gas analysis measured at time of sacrifice were within the acceptable range provided by The Ohio State University Veterinary Medical College whose Pathology Core performed the analysis and in agreement with canine stroke review of physiological parameters ([Fig. 1F](#)) [12]. Not surprisingly as immune cell infiltration has been reported as early as 30 min after MCAO, white blood cell count (WBC) at sacrifice was significantly increased compared to baseline in every hound ([Fig. 1G](#), $p < .0013$). Although platelet count decreased compared to baseline in all subjects, it remained insignificant ([Fig. 1H](#)). In order to demonstrate that the autologous clots that we prepared were clinically comparable, we performed immunofluorescent staining for VWF, fibrinogen, and platelet content on autologous clots prepared identically to those placed in the canine MCAO ([Fig. 1I](#)) [11,13,14]. Clots scanned at high resolution and quantified with Image J software contained $19.40 \pm 3.66\%$ fibrinogen (green), and $28.93 \pm 4.41\%$ VWF (violet), demonstrating comparable protein levels to published AIS LVO clots extracted from patients who have had mechanical thrombectomy retrieval [11,13]. After baseline DSA was established ([Fig. 2A–B](#)), consistent and sustained MCAO with TICI score of 0 was observed in all 6 hounds with no evidence of microemboli throughout injury, MRI, and transport up to 9 h after ischemic insult ([Fig. 2C–F](#)). We found no evidence of spontaneous recanalization, clot autolysis, or intracranial perforation. The mean infarct volume measured by MRI was $47.0 \pm 6.7\%$ of the ipsilateral hemisphere ($n = 6$). Maximal projection intensity of time of flight magnetic resonance angiography (TOF MRA) was used in the dorsal orientation to indicate lack of blood flow at the occluded MCA in all 6 hounds ([Fig. 3A](#)). Hyperintensities of the cerebral cortex were identified and consistent across coronal sections with T2-weighted imaging ([Fig. 3B–C](#)). DWI sequences (Figure D–E) showed hyperintense lesions indicative of reduced diffusion as seen in cytotoxic edema with corresponding hypointense lesions on ADC maps. Vasogenic edema which is extracellular will appear hyperintense on an ADP map. ([Fig. 3F–G](#)). TTC staining to identify between metabolically active and inactive regions of coronal sections mirrored infarction area in comparable regions ([Fig. 3H](#)). Hematoxylin and eosin staining confirmed MRI analyses with no evidence of subarachnoid hemorrhage in the medial section ([Fig. 3I](#)).

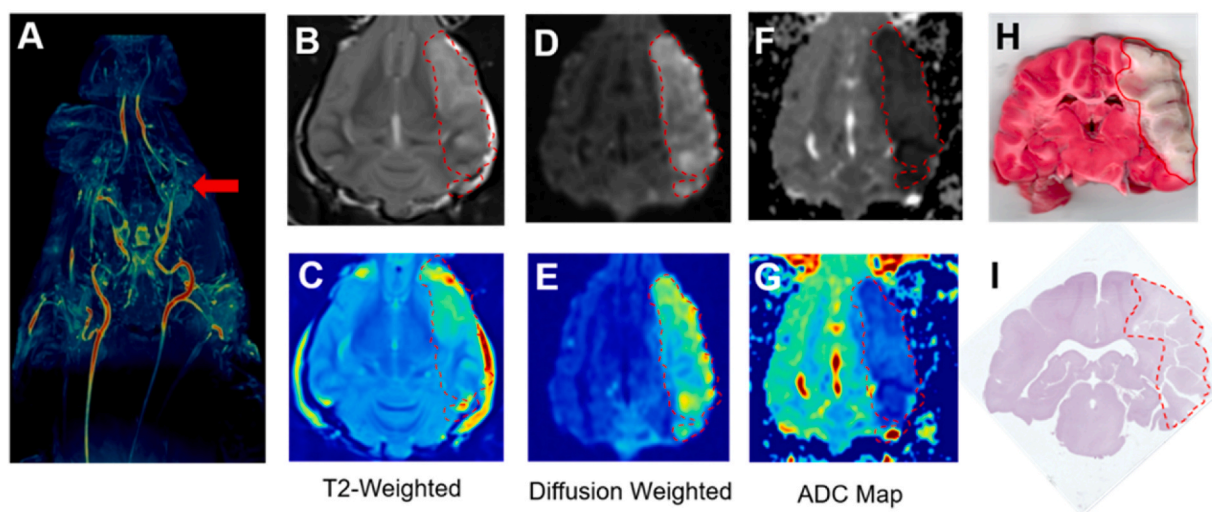


Fig. 3. Representative Canine MCAO Imaging and Histopathology. (A) TOF-MRA image in dorsal orientation of a representative hound with relevant arteries and collaterals demonstrating occlusion of middle cerebral artery (red arrow). (B,C) T2 weighted images in grayscale and pseudocolor demonstrating hyperintense lesion formation in the left MCA territory. (D,E) Final DWI in grayscale and pseudocolor showing an MCA territory infarct. (F,G) Corresponding hypointense lesions on ADC in grayscale and pseudocolor maps. (H) TTC stained coronal brain section identifying areas in red that are still metabolically active compared to white inactive regions 9 h after MCAO. (I) Hematoxylin and eosin stained coronal brain section with no evidence of hemorrhage.

4. Discussion

Although this manuscript is by no means a review, brief comparison of this large animal models with previous publications is appropriate. The preclinical model of LVO stroke presented approaching the MCA from posterior circulation has significant advantages. First, there are several different canine stroke occlusion models in addition to permanent and transient MCAO including the ICA, basilar artery, and vertebral artery occlusions previously published [2]. We occluded the MCA as the vast majority of AIS LVO occurs in this vessel clinically affecting the ipsilateral cortex with origin and branching of this vessel similar in both humans and dogs [6]. Secondly, our animal of choice for an AIS LVO model was the canine, specifically hounds. Mice, rats, cats, sheep, pigs, and non-human primate models are also utilized to study ischemic stroke; with rat, rabbit, and canine models favored for focal embolic and thromboembolic occlusion [6]. We originally began the characterization of this new posterior access MCAO large animal model in beagles. All attempts at LVO with these method in beagles resulted in perforation of cerebral vessels. Although the mean arterial wall thickness in canines is smaller than human arteries, approximately 2.5 mm compared to 3.0 mm, we quickly ascertained that hounds at approximately 3 times the body weight of beagles afforded the ample vessel diameter increase necessary to accommodate endovascular devices consistently [11]. Canines also offer a larger blood volume for multiple draws and a larger gyrencephalic brain size which results in optimal resolution with MRI with incidence of vasospasm comparable to humans [15–17]. In addition, a major limitation of both sheep and pig models, is the presence of a well-developed carotid rete mirabile providing collateral supply to the intracranial circulation, significantly impeding the ability to advance catheters into the MCA [3,4,18]. Gounis et al. described a rabbit model in which luminal stenosis was created in addition to injection of allogeneic clot into rabbit ICA to evaluate in vivo revascularization with intra-arterial fibrinolytic therapy and mechanical clot disruption with stent retriever [19]. However, the authors were primarily interested in the ability of the model to permit thromboembolic occlusion, and did not evaluate stroke volume or ischemia. Third, with regards to large animal AIS models aimed at studying transient as opposed to permanent occlusion there has been concern for poor reproducibility and spontaneous reperfusion with transient occlusion models [5,20,21]. Our model resulted in neither. Fourth, we chose to place an autologous clot with no additional chemical or physical accelerants or manipulations. During development of our model, we tested several previously utilized methods to create an autologous clot including the addition of thrombin and barium sulfate to attempt to recapitulate clinical AIS conditions, but arrived at the conclusion that static whole blood left at room temperature for 60 min led to clearer MR and angiogram imaging and more stable clots due to reduced serum content and clot retraction [5,14,21–24]. With this clot preparation, we saw no indication of clot lysis in the time after placement to sacrifice. In another study which used an autologous clot in a canine stroke model, whole blood was pulled the day before & left to sit overnight. The next day, clots were cut into 0.5–1 mm long sections and mixed with saline before injection into the ICA. Inter-arterial injection of tPA was attempted in 4 dogs and ¼ tPA treated dogs resulted in perfusion improvement [25]. Another study, also inducing clot formation with thrombin rested the clot overnight, and although the clot was not analyzed for constituents, based on our results we hypothesize that the clot content was not comparable to ours in VWF or platelet content [26]. Although barium addition to autologous blood resulted in stratification similar as to what is seen clinically, only part of the clot was fibrin rich, a downstream filter had to be placed and stabilization was not determined as occlusion was only accessed out to 45 min [23]. Brooks et al. previously developed an autologous clot stable enough to be consistently resected after canine LVO stroke with mechanical thrombectomy, but had to process the clot with citric acid, sodium citrate, dextrose solution, fibrinogen, thrombin and calcium chloride, which can affect the physiological architecture of this induced thrombus and potentially affect the therapeutic investigation [3,27]. Jiang et al., 2019 induced thrombus formation in autologous blood by adding thrombin but placed two clots in the MCAO, distal & proximal from the catheter, which resulted in 10–20% spontaneous reperfusion before treatment [28]. Fifth, many procedures to create animal models of AIS include craniotomy/craniectomy access in which microvascular clips, monofilaments, surgical suture, balloons, photochemical reactions, coils, and particles, to create occlusion [4,29]. Not only is it important to have a model in which the material used to create occlusion is accessible to the therapeutic drug of interest, but endovascular occlusion using autologous blood is minimally invasive compared to removing the skull which introduces additional physical injury including drill injury, thermal damage, change in brain temperature, decreased CSF volume, lower cranial pressure, and resulting edema making both species undesirable for a large animal AIS LVO model [6,18,30–32]. Surprisingly, most focal ischemic strokes are caused by thromboembolism, yet the vast majority of models utilized filaments, balloons, or coil occlusion which, while they recapitulate the ischemia-reperfusion phenomenon of LVO stroke, are not suitable for thrombolytic or thrombectomy drug studies [8,33,34]. In addition, few of these experimental animal models have demonstrated the ability to prolong a non-survival experimental ischemic period within physiological parameters outside the standard 4.5 h thrombolytic rtPA treatment window with or without an autologous clot [4,33]. The inherent issue with filament and synthetic silicon or rubber fillers is that human ischemic stroke rarely results in complete and stable vessel occlusion with the majority of patients experiencing spontaneous reperfusion and successive resolution in the first 48 h after onset which negates use of these models by etiology from all three major subtypes of stroke [15,32,35–37]. The intraluminal suture model results in high variability in lesion volume and location across and within studies in both small and large animals. Real time placement of an occluder in rodent MCA cannot be visualized leading to overshooting or undershooting contributing to lesion variability and regardless of animal size, a major disadvantage of this model is premature reperfusion which occurs in 25% of experimental animals [17]. The inherent issue with AIS models which utilize crush, chemical, electrocautery, or laser injury is that although they do replicate a platelet rich arterial thrombus, they cannot be used to study clinically relevant reperfusion [6,38]. Transient vessel occlusion allows study of reperfusion effects but hemodynamic characteristics are different from those seen in reperfusion. Using blood clots for vessel occlusion perfectly simulates the pathophysiological mechanism of human stroke, is minimally invasive, and allows study of thrombolysis or anti-coagulative interventions [39]. Finally, the use of synthetic materials for occlusion also raises the question of similarity to stroke onset in humans given that focal ischemia generally occurs in relation to either thrombi or emboli composed of platelets and/or fibrin into the MCA [24]. Our autologous clot was

similar in both VWF and fibrin content to clots resected from AIS LVO patients by mechanical thrombectomy [11].

Our model could be used to compare with the clinical protocol currently utilized for rTPA administration AFTER its proven window of efficacy and safety. Whether our MCAO model is suitable for prophylactic or thrombolytic studies with 9 h after occlusion and/or whether this model can be utilized for the study of endovascular thrombectomy remains to be demonstrated and is our current line of investigation.

The model we established does have some disadvantages. First, although canines are less expensive than NHP, the procurement, shipping, per diem, and surgical costs are significant and even higher in hounds compared to beagles. Even though aged canines would be more appropriate for AIS LVO studies considering the patient population commonly affected, we could not get adult hounds in sufficient numbers from any vendor. In addition, catheters and guidewires added appreciable costs to large animal neurovascular access and in our hands, the Synchro 2 soft 0.014" guidewire and Headway 17 advanced into the MCAO most smoothly, offering the least resistance and resulting in little to no vasospasm and adequate speed to desired clot placement location. Secondly, a more proximal LVO arterial location such as the carotid or basilar artery are easier to access as significant tortuosity is present in the ICA and increased risk of vasospasm may compromise the ability to re-access the vessel again or iatrogenic increase in stroke volume [18,33,34]. Third, we did not use any additional antiplatelet or anticoagulants which AIS LVO patients may already have on board at diagnosis nor did our model take into consideration hypertension, both conditions common in this patient population. Fourth, we used intravenous anesthesia for induction and inhalants for maintenance which may not be optimal for all therapeutic investigations. Our reasoning was to reduce stress on the canine at the beginning of the procedures and allow immediate augmentation through intravenous administration if needed during transport to and from MRI. Isoflurane for maintenance allowed a second assistant to the surgeon to "fine tune" the subject's depth of anesthesia during catheter manipulations when the surgeon had no free hands, increasing the percentage of isoflurane with a quick twist of the vaporizer. Fifth, one major restriction which must be considered is the extensive collateral circulation of canine cerebral arteries which limits stroke size [3,18]. Just as important, in humans, white matter constitutes 60% of the brain whereas it comprises only 35% dogs, but still preferable to rodents where white matter is only 10–15% of the brain [32]. Sixth, a steep learning curve to access the MCA endovascularly and common vasospasm results in considerable speed of advancement to MCA origin [17]. We decreased this confounder greatly by utilizing a vascular neurosurgeon with extensive experience to access the MCA in each canine. Lastly, this study presented a small sample size. We would caution the generalization of our results, although the vast majority of neurointerventional large animal models publish less than 10 animals/group with an average of 6 in canine studies. Low infarction volume variability by MRI have been completed with as little as 3 canines per experimental group [17,39].

5. Conclusion

This study describes a reproducible large animal LVO stroke, as demonstrated on both DSA and MRI and verified by histopathology. It differs from other large animal and specifically canine LVO stroke models as we used posterior access and an untreated autologous clot to establish occlusion which remained stable over prolonged induced ischemia. To our knowledge, this study is the only published LVO large animal stroke model which resulted in 100% success rate of MCA occlusion with an autologous clot with no added coagulants and no spontaneous reperfusion throughout 9 h of ischemia.

Author contribution statement

Debra Wheeler; Amanda S. Zakeri: Performed the experiments; Analyzed and interpreted the data; Wrote the paper. Allyson Huttinger; Arianna Carfora; Aarushi Kini; Taggart Stork; Simon Yacoub; Cole Anderson: Performed the experiments; Analyzed and interpreted the data. Matthew Joseph; Mohammed T. Shujaat: Performed the experiments; Analyzed and interpreted the data; Contributed reagents, materials, analysis tools or data. Shahid M. Nimjee: Conceived and designed the experiments; Performed the experiments; Analyzed and interpreted the data; Contributed reagents, materials, analysis tools or data.

Funding statement

Shahid M. Nimjee was supported by NHLBI Division of Intramural Research [1R44HL152869].

Data availability statement

Data included in article/supplementary material/referenced in article.

Declaration of interest's statement

The authors declare that they have no known competing financial interests or personal relationships that could have appeared to influence the work reported in this paper.

References

- [1] GBD 2016 Risk Factors Collaborators, Global, regional, and national comparative risk assessment of 84 behavioural, environmental and occupational, and metabolic risks or clusters of risks, 1990–2016: a systematic analysis for the Global Burden of Disease Study 2016, *Lancet* 390 (10100) (2017 Sep 16) 1345–1422. Erratum in: *Lancet*. 2017 Oct 14;390(10104):1736. Erratum in: *Lancet*. 2017 Oct 28;390(10106):e38.
- [2] H. Handelsmann, L. Herzog, Z. Kulcsar, A.R. Luft, S. Wegener, Predictors for affected stroke territory and outcome of acute stroke treatments are different for posterior versus anterior circulation stroke, *Sci. Rep.* 11 (1) (2021 May 18), 10544.
- [3] M.S. Shazeeb, R.M. King, O.W. Brooks, A.S. Puri, N. Henninger, J. Boltze, M.J. Gounis, Infarct evolution in a large animal model of middle cerebral artery occlusion, *Transl Stroke Res* 11 (3) (2020 Jun) 468–480.
- [4] E.E. Kaiser, F.D. West, Large animal ischemic stroke models: replicating human stroke pathophysiology, *Neural Regen. Res.* 15 (8) (2020 Aug) 1377–1387. Gillilan LA. Extra- and intra-cranial blood supply to brains of dog and cat. *Am J Anat* 1976;146(3):237–53.[published Online First: 1976/07/01].
- [5] Y. Li, J. Zhang, Animal models of stroke, *Anim. Models Exp. Med.* 4 (3) (2021 Sep 15) 204–219.
- [6] A. Taha, J. Bobi, R. Dammers, et al., Comparison of large animal models for acute ischemic stroke: which model to use? *Stroke* (2022), STROKEAHA121036050 [published Online First: 2022/02/16].
- [7] Gnyawali SC, Wheeler DG, Huttinger AL, et al. Quantification of cerebral perfusion using laser speckle imaging and infarct volume using MRI in a pre-clinical model of posterior circulation stroke. *J. Vis. Exp.* 2020(165) [published Online First: 2020/12/08].
- [8] A.L. Huttinger, D.G. Wheeler, S. Gnyawali, D. Dornbos 3rd, J.M. Layzer, N. Venetos, S. Talentino, N.J. Musgrave, C. Jones, C. Bratton, M.E. Joseph, C. Sen, B. A. Sullenger, S.M. Nimjee, Ferric chloride-induced canine carotid artery thrombosis: a large animal model of vascular injury, *J. Vis. Exp.* (139) (2018 Sep 7), 57981.
- [9] S.A. Arnold, S.R. Platt, K.P. Gendron, F.D. West, Imaging ischemic and hemorrhagic disease of the brain in dogs, *Front. Vet. Sci.* 7 (2020 May 27) 279.
- [10] R.T. Higashida, A.J. Furlan, H. Roberts, T. Tomsick, B. Connors, J. Barr, W. Dillon, S. Warach, J. Broderick, B. Tilley, D. Sacks, Technology assessment committee of the American society of interventional and therapeutic neuroradiology; technology assessment committee of the society of interventional radiology. Trial design and reporting standards for intra-arterial cerebral thrombolysis for acute ischemic stroke, *Stroke* 34 (8) (2003 Aug) e109–e137. Epub 2003 Jul 17. Erratum in: *Stroke*. 2003 Nov;34(11):2774.
- [11] L. Di Meglio, J.P. Desilles, V. Ollivier, M.S. Nomenjanahary, S. Di Meglio, C. Deschildre, S. Loyau, J.M. Olivot, R. Blanc, M. Piotin, M.C. Bouton, J.B. Michel, M. Jandrot-Perrus, B. Ho-Tin-Noé, M. Mazighi, Acute ischemic stroke thrombi have an outer shell that impairs fibrinolysis, *Neurology* 93 (18) (2019 Oct 29) e1686–e1698. Epub 2019 Sep 20. Erratum in: *Neurology*. 2019 Oct 29;93(18):819.
- [12] Keagan J. Boustead, Justin F. Grace, Roxanne K. Buck, Gareth E. Zeiler, Comparative effects of three different ventilatory treatments on arterial blood gas values and oxygen extraction in healthy anaesthetized dogs, *Vet. Anaesth. Analg.* 49 (3) (2022) 251–264.
- [13] O.M. Mereuta, M. Abbasi, S. Fitzgerald, D. Dai, R. Kadirvel, R.A. Hanel, A.J. Yoo, M.A. Almekhlafi, K.F. Layton, J.E. Delgado Almandoz, P. Kvamme, V. Mendes Pereira, B.S. Jahromi, R.G. Nogueira, M.J. Gounis, B. Patel, A. Aghaebrahim, E. Sauvageau, P. Bhuvu, J. Somro, A.M. Demchuk, I.C. Thacker, Y. Kayan, A. Copelan, P. Nazari, D.R. Cantrell, D.C. Haussen, A.R. Al-Bayati, M. Mohammad, L. Pisani, G.M. Rodrigues, A.S. Puri, J. Entwistle, A. Meves, J.L. Arturo Larco, L. Savastano, H.J. Cloft, D.F. Kallmes, K.M. Doyle, W. Brinjikji, Histological evaluation of acute ischemic stroke thrombi may indicate the occurrence of vessel wall injury during mechanical thrombectomy, *J. Neurointerventional Surg.* 14 (4) (2022 Apr) 356–361. Epub 2021 May 11.
- [14] S.H. Lee, S.W. Kim, J.M. Kim, W.C. Son, In vivo evaluation of histopathologic findings of vascular damage after mechanical thrombectomy with the Tromba device in a canine model of cerebral infarction, *PLoS One* 17 (10) (2022 Oct 14), e0276108.
- [15] M. Mehra, N. Henninger, J.A. Hirsch, J. Chueh, A.K. Wakhloo, M.J. Gounis, Preclinical acute ischemic stroke modeling, *J. Neurointerventional Surg.* 4 (4) (2012 Jul) 307–313.
- [16] Q.Q. Zu, S. Liu, X.Q. Xu, S.S. Lu, L. Sun, H.B. Shi, An endovascular canine stroke model: middle cerebral artery occlusion with autologous clots followed by ipsilateral internal carotid artery blockade, *Lab. Invest.* 93 (7) (2013 Jul) 760–767.
- [17] C. Rink, G. Christoforidis, A. Abduljalil, M. Kontzialis, V. Bergdall, S. Roy, S. Khanna, A. Slivka, M. Knopp, C.K. Sen, Minimally invasive neuroradiologic model of preclinical transient middle cerebral artery occlusion in canines, *Proc. Natl. Acad. Sci. U. S. A.* 105 (37) (2008 Sep 16) 14100–14105. Epub 2008 Sep. 8.
- [18] K. Atchaneeyasakul, L. Guada, K. Ramdas, M. Watanabe, P. Bhattacharya, A.P. Raval, D.R. Yavagal, Large animal canine endovascular ischemic stroke models: a review, *Brain Res. Bull.* 127 (2016 Oct) 134–140. Epub 2016 Aug 3.
- [19] M.J. Gounis, A.K. Wakhloo, J.Y. Chueh, Preclinical investigations for thrombectomy devices—does it translate to humans? *Stroke* 44 (6 Suppl 1) (2013 Jun) S7–S10.
- [20] M. Bacigaluppi, G. Comi, D.M. Hermann, Animal models of ischemic stroke. Part two: modeling cerebral ischemia, *Open Neurol. J.* 4 (2010 Jun 15) 34–38.
- [21] A. Shaibani, S. Khawar, W. Shin, T.A. Cashen, B. Schirf, M. Rohany, S. Kakodkar, T.J. Carroll, First results in an MR imaging-compatible canine model of acute stroke, *AJNR Am J Neuroradiol* 27 (8) (2006 Sep) 1788–1793.
- [22] A.S. Boulos, E.M. Deshaies, J.C. Dalfino, P.J. Feustel, A.J. Popp, D. Drazin, Tamoxifen as an effective neuroprotectant in an endovascular canine model of stroke, *J. Neurosurg.* 114 (4) (2011 Apr) 1117–1126. Epub 2010 Oct 1.
- [23] Y. Zhang, M. Jin, B. Du, H. Lin, C. Xu, W. Jiang, J. Jia, A novel canine model of acute vertebral artery occlusion, *PLoS One* 10 (11) (2015 Nov 6), e0142251.
- [24] Y.Z. Ma, L. Li, J.K. Song, Z.R. Niu, H.F. Liu, X.S. Zhou, F.S. Xie, G.H. Du, A novel embolic middle cerebral artery occlusion model induced by thrombus formed in common carotid artery in rat, *J. Neurol. Sci.* 359 (1–2) (2015 Dec 15) 275–279. Epub 2015 Oct 5.
- [25] A.D. Harris, J.C. Kosior, R.C. Ryder, L.B. Andersen, W.Y. Hu, M. Hudon, W.H. Morrish, R.J. Sevick, J. Wong, R. Frayne, MRI of ischemic stroke in canines: applications for monitoring intraarterial thrombolysis, *J. Magn. Reson. Imag.* 26 (6) (2007 Dec) 1421–1428. Erratum in: *J Magn Reson Imaging*. 2008 Oct;28(4): 1053.
- [26] M.J. Gounis, R.G. Nogueira, M. Mehra, J. Chueh, A.K. Wakhloo, A thromboembolic model for the efficacy and safety evaluation of combined mechanical and pharmacologic revascularization strategies, *J. Neurointerventional Surg.* 5 (Suppl 1) (2013 May) i85–i89. Epub 2012 Sep. 8.
- [27] O.W. Brooks, R.M. King, E. Nossek, M. Marosfoi, J. Caroff, J.Y. Chueh, A.S. Puri, M.J. Gounis, A canine model of mechanical thrombectomy in stroke, *J. Neurointerventional Surg.* 11 (12) (2019 Dec) 1243–1248. Epub 2019 May 18.
- [28] R.H. Jiang, Q.Q. Zu, X.Q. Xu, B. Wang, Y. Ding, J. Wang, S. Liu, H.B. Shi, A canine model of hemorrhagic transformation using recombinant tissue plasminogen activator administration after acute ischemic stroke, *Front. Neurol.* 10 (2019 Jun 25) 673.
- [29] N. Saadat, G.A. Christoforidis, Y.I. Jeong, M. Liu, A. Dimov, S. Roth, M. Niekraz, S.A. Ansari, T. Carroll, Influence of simultaneous pressor and vasodilatory agents on the evolution of infarct growth in experimental acute middle cerebral artery occlusion, *J. Neurointerventional Surg.* 13 (8) (2021 Aug) 741–745. Epub 2020 Sep. 8.
- [30] L.A. Gillilan, Extra- and intra-cranial blood supply to brains of dog and cat, *Am. J. Anat.* 146 (3) (1976 Jul) 237–253.
- [31] J. Gralla, G. Schroth, L. Remonda, A. Fleischmann, J. Fandino, J. Slotboom, C. Brekenfeld, A dedicated animal model for mechanical thrombectomy in acute stroke, *AJNR Am. J. Neuroradiol.* 27 (6) (2006 Jun-Jul) 1357–1361.
- [32] C.J. Sommer, Ischemic stroke: experimental models and reality, *Acta Neuropathol.* 133 (2) (2017 Feb) 245–261. Epub 2017 Jan 7.
- [33] G.A. Christoforidis, C. Rink, M.S. Kontzialis, Y. Mohammad, R.M. Koch, A.M. Abduljalil, V.K. Bergdall, S. Roy, S. Khanna, A.P. Slivka, M.V. Knopp, C.K. Sen, An endovascular canine middle cerebral artery occlusion model for the study of leptomeningeal collateral recruitment, *Invest. Radiol.* 46 (1) (2011 Jan) 34–40. PMID: 20856126.
- [34] G.A. Christoforidis, N. Saadat, M. Liu, Y.I. Jeong, S. Roth, M. Niekraz, T. Carroll, Effect of early Sanguinate (PEGylated carboxyhemoglobin bovine) infusion on cerebral blood flow to the ischemic core in experimental middle cerebral artery occlusion, *J. Neurointerventional Surg.* 14 (12) (2022 Dec) 1253–1257. Epub 2021 Dec 14.
- [35] B.T. Kang, D.P. Jang, S.H. Gu, J.H. Lee, D.I. Jung, C.Y. Lim, H.J. Kim, Y.B. Kim, H.J. Kim, E.J. Woo, Z.H. Cho, H.M. Park, MRI features in a canine model of ischemic stroke: correlation between lesion volume and neurobehavioral status during the subacute stage, *Comp. Med.* 59 (5) (2009 Oct) 459–464.

- [36] J.H. Jeon, H.W. Jung, H.M. Jang, J.H. Moon, K.T. Park, H.C. Lee, H.Y. Lim, J.H. Sur, B.T. Kang, J. Ha, D.I. Jung, Canine model of ischemic stroke with permanent middle cerebral artery occlusion: clinical features, magnetic resonance imaging, histopathology, and immunohistochemistry, *J. Vet. Sci.* 16 (1) (2015) 75–85. Epub 2014 Sep. 30.
- [37] G.F. Molinari, Experimental cerebral infarction. I. Selective segmental occlusion of intracranial arteries in the dog, *Stroke* 1 (4) (1970 Jul-Aug) 224–231.
- [38] P.D. Purdy, M.D. Devous Sr., H.H. Batjer, C.L. White 3rd, Y. Meyer, D.S. Samson, Microfibrillar collagen model of canine cerebral infarction, *Stroke* 20 (10) (1989 Oct) 1361–1367.
- [39] A.M. Herrmann, S. Meckel, M.J. Gounis, L. Kringe, E. Motschall, C. Mülling, J. Boltze, Large animals in neurointerventional research: a systematic review on models, techniques and their application in endovascular procedures for stroke, aneurysms and vascular malformations, *J. Cerebr. Blood Flow Metabol.* 39 (3) (2019 Mar) 375–394. Epub 2019 Feb 7.